Original Article

Development of fetal magnetic resonance imaging (MRI) phantom

Marina Valeryevna Cherkasskaya[1]^, Egor Mikhailovich Syrkashev[1,2]^, Maria Valerievna Sokolova[1]^, Alexey Vladimirovich Petraikin[1]^, Dmitry Sergeevich Semenov[1]^, Yuri Aleksandrovich Vasilev[1]^

[1]State Budget-Funded Health Care Institution of the City of Moscow "Research and Practical Clinical Center for Diagnostics and Telemedicine Technologies of the Moscow Health Care Department", Moscow, the Russian Federation; [2]FSBI "National Medical Research Center for Obstetrics, Gynecology and Perinatology Named after Academician V.I.Kulakov", Moscow, the Russian Federation

Contributions: (I) Conception and design: EM Syrkashev; (II) Administrative support: YA Vasilev; (III) Provision of study materials or patients: MV Cherkasskaya, DS Semenov; (IV) Collection and assembly of data: MV Sokolova; (V) Data analysis and interpretation: AV Petraikin; (VI) Manuscript writing: All authors; (VII) Final approval of manuscript: All authors.

Correspondence to: Marina Valeryevna Cherkasskaya, PhD. State Budget-Funded Health Care Institution of the City of Moscow "Research and Practical Clinical Center for Diagnostics and Telemedicine Technologies of the Moscow Health Care Department", 24 Building 1 Petrovka St., Moscow 127051, the Russian Federation. Email: rylkovamarina@yandex.ru.

Background: Anthropomorphic phantoms play an important role in routine clinical practice. They can be used to calibrate magnetic resonance imaging (MRI) scanners, control the diagnostic equipment quality, and reduce the acquisition time. The latter is especially critical for diagnosing fetal anomalies, which requires optimal image quality within the shortest possible time. This paper aims to develop an MRI fetal phantom and determine the materials that best mimic the magnetic resonance (MR) characteristics of its internal organs. Future phantom features will include simulations of fetal limb movements.

Methods: A single MRI study of a pregnant woman at 20 weeks 3 days of gestation was used as a reference and for image segmentation. Anonymized Digital Imaging and Communication in Medicine (DICOM) files were imported into 3D Slicer v. 5.2.1 for segmentation of the uterus, fetus, and internal organs. Based on the performed segmentation, a three-dimensional model was obtained for printing on a 3D printer. The mold was 3D printed on an Anycubic Photon M3 Max printer. The paper showcases the selection and manufacturing of compositions to simulate the relaxation times of the fetal organs. Formulations for emulsions and carrageenan- and agar-based hydrogels are presented. The selected compositions were used to fill the 3D printed model.

Results: Statistical analysis showed no significant differences in absolute and relative signal values obtained from scans of a pregnant woman at 20 weeks and 3 days and a fetal phantom.

Conclusions: During the study, an anthropomorphic fetal phantom was constructed, filled with compositions with relaxation times T1 and T2 similar to the control values of the corresponding tissues. The phantom can be used to set up and optimize fetal MRI protocols, train and educate medical students, residents, graduate students, and X-ray technicians, as well as to timely control image quality and equipment serviceability.

Keywords: Fetal magnetic resonance imaging (fetal MRI); phantom; tissue-mimicking materials; hydrogels; three-dimensional printing (3D printing)

^ ORCID: Marina Valeryevna Cherkasskaya, 0000-0003-4952-1619; Egor Mikhailovich Syrkashev, 0000-0003-4043-907X; Maria Valerievna Sokolova, 0009-0005-3689-3810; Alexey Vladimirovich Petraikin, 0000-0003-1694-4682; Dmitry Sergeevich Semenov, 0000-0002-4293-2514; Yuri Aleksandrovich Vasilev, 0000-0002-5283-5961.

Submitted Mar 13, 2024. Accepted for publication Jul 10, 2024. Published online Aug 28, 2024.
doi: 10.21037/qims-24-501
View this article at: https://dx.doi.org/10.21037/qims-24-501

Introduction

Magnetic resonance imaging (MRI) is a highly accurate diagnostic method capable of assessing fetal congenital malformations, as well as the abdominal cavity and pelvis of a pregnant woman (1,2). The absence of ionizing radiation, combined with high contrast and spatial resolution, makes MRI a valuable complement to ultrasound evaluating various pathological conditions in pregnant women and fetuses (3-6).

However, MRI has certain limitations, including a relatively long turnaround time during which the pregnant woman has to remain motionless. This procedure relies on established scanning protocols designed to achieve adequate image quality within the shortest possible time. Additionally, spontaneous movements by the fetus and mother can generate clinically significant artifacts that compromise exam interpretation (7). To minimize these limitations, phantoms can help configure and practice pulse sequences as needed, eliminating the need for pregnant patients to participate. Furthermore, phantom studies enable testing of existing scanning protocols and standardizing data collection.

The literature describes previous developments of fetal phantoms for MRI, but many have limitations. Some have primitive designs (8), lack anatomical accuracy (9), or are designed to simulate blood circulation (10-12). For example, a test object designed to test the distribution of signal-to-noise ratios in the abdominal cavity of a pregnant woman closely resembled the dimensions and shapes of the target organ and was filled with a solution whose signal is comparable to that of a human body. However, it failed to reflect the topographic anatomy of a pregnant woman's abdomen (13). Another group created a fetal phantom using containers filled with oil, water, and an oil-in-water multi-component fat emulsion, surrounded by bags of saline solution and placed inside a phantom simulating a pregnant woman (14). Despite the ingenious design, the phantoms lacked anthropomorphic features, limiting their effectiveness for fetal imaging.

Typically, phantoms are made to mimic one or several properties of human organs. The reason is, that various types of biological objects possess distinct magnetic resonance (MR) features because of complex structure and chemical composition. Simulation models must be made of safe and non-toxic materials capable of retaining their structure and properties over time. MRI phantoms must realistically mimic spin-lattice (T1) and spin-spin (T2) relaxation times. This study focuses on the test objects that mimic the relaxation times of human tissues. Such objects open the way to reducing the turnaround time by fine-tuning the sequences to create an optimized acquisition protocol (15). To achieve this, gel-like structures such as agarose (16), gelatine, carrageenan, polyacrylamide, and polyvinyl alcohol are often used (17). The broad availability of these components stems from the ease of fabrication, adequate mechanical resistance, and the ability to imitate most body tissues (18). One group demonstrated how the concentration of gelling and contrast agents affected the relaxation times of gels when creating phantoms with a specific set of features (19). The transverse relaxation time T2 can be adjusted by fine tuning the hydrogel concentration (20-22). Paramagnetic additives such as nickel sulphate, nickel chloride, or gadolinium-based contrast agents are typically added to alter the longitudinal relaxation time T1 (23). Agarose gels doped with paramagnetic additives are used to mimic the brain, muscles, liver, and spleen (24-26). Agarose combined with carrageenan and gadolinium (III) chloride can be used to mimic muscle tissues (27). Adjusting the concentration of agarose and gadolinium (III) chloride in the mixture makes it possible to simulate the relaxation time of human tissues (28).

It is possible to fabricate phantoms of complex geometric shapes and reduce the modelling time using three-dimensional (3D) printing to construct a phantom body that can be filled with tissue surrogates. In (29), the authors 3D-printed a uterus with hollow compartments for the embryo and maternal organs and filled it with agarose gels. The authors simulated a woman's body, uterus, placenta, and the fetus' brain and body at 36 weeks gestation. This approach to manufacturing a test object is used in the current study. This paper aims to develop an MRI fetal phantom and determine the materials that best mimic the MR characteristics of its internal organs. We present this article in accordance with the MDAR reporting checklist (available at https://qims.amegroups.com/article/view/10.21037/qims-24-501/rc).

Table 1 MRI acquisition parameters

MRI pulse sequence	TR (ms)	TE (ms)	FOV (mm)	Matrix	Slice thickness (mm)
T2WI	11,520	130	350×350	256×256	4
T1WI	126	4	350×300	256×160	4
T2WI FS	7,500	130	350×350	256×256	4

MRI, magnetic resonance imaging; TR, repetition time; TE, short echo time; FOV, field of view; T2WI, T2 weighted image; T1WI, T1 weighted image; T2WI FS, T2 weighted image with fat suppression.

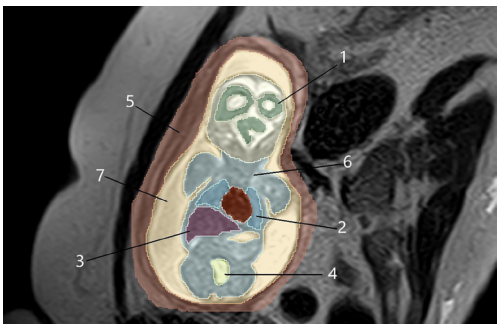

Figure 1 An example of ROIs on coronal T2WI images identified using 3D Slicer software: 1, white matter; 2, lung; 3, liver; 4, bladder; 5, maternal muscles; 6, fetal muscles; 7, amniotic fluid. ROI, region of interest; T2WI, T2-weighted image; 3D, three-dimensional.

Methods

As the Russian healthcare system provides the second screening at 18–21 weeks of pregnancy, there is a large number of fetal MRI studies available for this gestational age. A single MRI study of a pregnant woman at 20 weeks 3 days was chosen to serve as a reference and for image segmentation. The study was conducted in accordance with the Declaration of Helsinki (as revised in 2013). The study was approved by independent ethics committee of State Budget-Funded Health Care Institution of the City of Moscow "Research and Practical Clinical Center for Diagnostics and Telemedicine Technologies of the Moscow Health Care Department" (N06/2023 from September 21, 2023). Digital Imaging and Communication in Medicine (DICOM) files was downloaded retrospectively from Unified Radiological Information Service. The segmentation and ROI identification were performed on the same study [T1, T2 and T2 with fat suppression (T2FS)] simultaneously. Since this study investigated an extragenital disease, a study of a physiological pregnancy was chosen as a source of initial images. Informed consent for the use of anonymized images for academic purposes was obtained.

All acquisitions for this study were performed using a 1.5 T Toshiba Excelart Vantage MRI scanner. The acquisition parameters corresponded to those used in routine practice for investigating fetal anomalies (*Table 1*). T2-weighted images (T2WI) were obtained using single-shot fast spin-echo (SS-FSE) sequences, while T1-weighted images (T1WI) were obtained using spin-echo (SE) sequences. MRI signal suppression from adipose tissue was performed using chemically selective saturation (CHESS).

DICOM files were anonymized and imported into 3D Slicer v. 5.2.1 for segmentation of the uterus, fetus, and internal organs (*Figure 1*). The regions of interest were contoured manually by a radiologist with 12 years of experience. To identify the regions of interest, T1, T2, and T2FS images in the coronal plane relative to the fetus were used. To determine the signal intensity of the tissue (SI_{tissue}) of interest, the most homogeneous areas were selected. Next, within each organ, 3 regions of interest were identified, and the average SI_{tissue} was calculated. This value was used as a reference when selecting suitable solutions. Additionally, we calculated the ratio between the SI_{tissue} of the region of interest and the SI_{saline} of an isotonic sodium chloride solution (saline) that simulated amniotic fluid in the phantom and was placed next to the pregnant woman during the acquisition according Eq. [1]. This was done to improve reproducibility, since 1.5 Tesla MRI scanners may differ in terms of absolute SI.

$$SI_{rel.tissue} = \frac{SI_{tissue}}{SI_{saline}} \quad [1]$$

Where $SI_{rel.tissue}$: relative MR signal of fetal tissue, relative units; SI_{tissue}: MR signal for fetal tissue; SI_{saline}: MR signal for saline.

To create the 3D model shape, manual segmentation of the uterus, fetus and its internal organs (maturing white matter of the brain, lungs, liver, stomach, bladder,

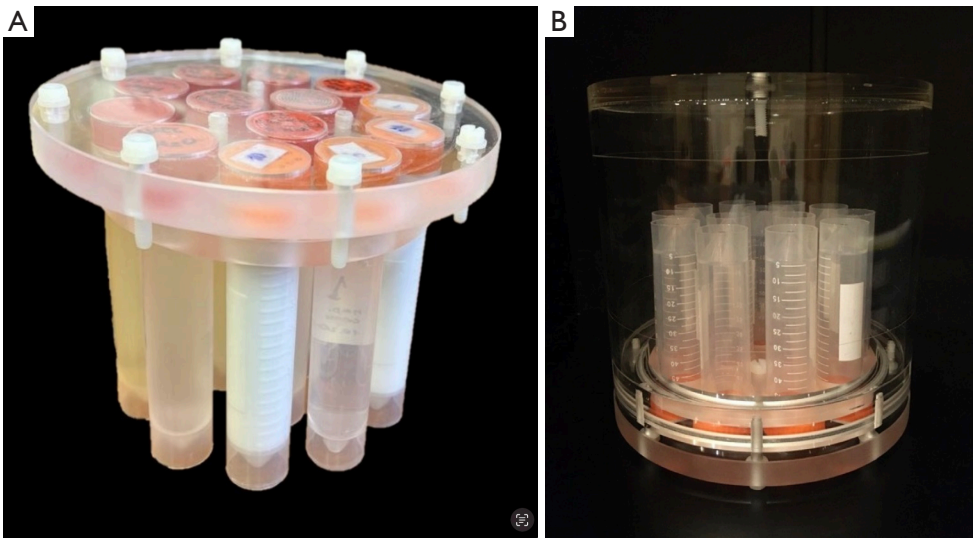

Figure 2 The inside of the phantom containing test tubes filled with test compounds (A); an assembled phantom (B).

muscles and amniotic fluid) was performed. The resulting segmentation was rendered into a three-dimensional model in the Compass-3D v21 software. The 3D model was then imported to the CHITUBOX V1.9.5 for the final processing and 3D printing.

The mold was 3D printed from Anycubic photopolymer resin on an Anycubic Photon M3 Max printer. The phantom lid was printed from ABS thermoplastic on a Picaso 3D Designer X PRO printer. 3D printing made it possible to achieve anatomical accuracy and replicate geometric distortions that occur during data acquisition, image processing, and model fabrication (30). The phantom comprises several stacks: the uterus, amniotic fluid, and the fetus with internal organs (maturing white matter of the brain, lungs, liver, stomach, bladder, and muscles). A lid was used to seal the phantom.

During the preliminary tailoring we prepared a series of hydrogel compositions based on 0.1%, 0.3%, 0.6%, 0.9%, 1.2%, 1.5%, 2%. (Agarose Basic, Product code: A5963, PanReac AppliChem ITW Reagents, Germany) and mixed them 1%, 2%, and 3% kappa-carrageenan (Product code: 5060341111983, Special Ingredients, UK). Degassed deionized water was heated to 50 ℃, and the agarose/carrageenan and agarose powders were added slowly. The mixture was heated to 60–75 ℃ and stirred on an Amtast MSH-2 magnetic stirrer (China). Once the gel had partially cooled down, the Gadovist® (ATC code: V08CA09, BAYER, AG, Germany) contrast agent was added. The mixture was mixed again and left to cool in the open. Once the gels had cooled down, they were refrigerated to ensure stability and prevent bacterial growth.

To mimic the maturing cortex and intermediate white matter of the brain, we prepared oil-in-water emulsions based on sunflower oil with fat phase concentrations of 20%, 40%, and 60%. To maintain the stability of the emulsions, the emulsifier Behentrimonium Methosulfate (Product code: S02700, Croda) was used. The emulsifier was heated, blended with vegetable oil, and dispersed using an IKA Ultra Turrax T 25 dispersing tool (Germany). The resulting emulsions were put into a refrigerator.

Solutions of paramagnetic salts imitating muscle tissue and the bladder were prepared by dissolving samples of 1.07 and 11.93 mM $NiCl_2$ (Product code: 8.06722, Sigma-Aldrich®), 0.20, and 0.30 mM $MnCl_2$ (Product code: 8.05930, Sigma-Aldrich®), in distilled water.

Before the MRI scan, all test compounds were poured into plastic tubes (*Figure 2*), hermetically sealed, labelled, and placed inside a cylindrical acrylic case filled with blank isotonic saline. Statistical analysis of the results was carried out in the Python programming language using the SciPy library.

Results

The objective of this study was to tailor the gel compositions to mimic the reference T1 and T2 relaxation times of the corresponding tissues. Axial MR images of the test compositions are presented in *Figure 3*.

To optimize the tissue-mimicking compositions, we

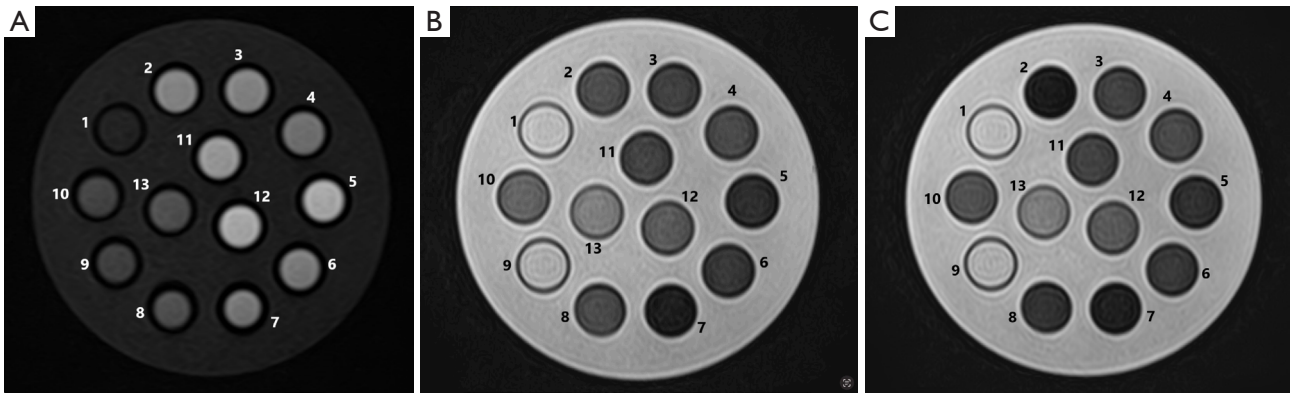

Figure 3 Test tubes in axial plane: (A) T1 WI; (B) T2 WI; (C) T2FS WI. Content of the tubes: 1, distilled water; 2, sunflower oil; 3, 1% agarose with 0.66 M contrast agent; 4, 1% agarose with 0.33 M contrast agent; 5, 3% carrageenan with 0.5% agarose and 0.33 M contrast agent; 6, 2% carrageenan with 0.5% agarose and 0.33 M contrast agent; 7, 0.2 mM $MnCl_2$; 8, emulsion with 60% fat phase; 9, 1.07 mM $NiCl_2$; 10, emulsion with 40% fat phase; 11, 1% carrageenan with 0.5% agarose and 0.33 M contrast agent; 12, 0.6% agarose with 0.33 M contrast agent; 13, 0.6% agarose with 0.33 M contrast agent. T1, spin-lattice relaxation time; WI, weighted image; T2, spin-spin relaxation time; T2FS, T2 with fat suppression; M, mole; mM, millimole; $MnCl_2$, manganese (II) chloride; $NiCl_2$, nickel (II) chloride.

built curves relating the relative MR signals on T1, T2, and T2FS-weighted images to the contrast agent with the same agarose concentration (0.3%):

$$\begin{aligned} y&=0.8886x-0.1112\\ y&=-0.1363x+1.2845;\\ y&=-0.1386x+1.3388 \end{aligned} \quad [2]$$

respectively, where x is the amount of contrast agent in µL, y is the relative signal (normalized to the isotonic NaCl solution).

Additional plots reflected the relationship between the relative MR signal on T1, T2, and T2FS-weighted images and the agarose concentration at 1 µL contrast agent:

$$\begin{aligned} y&=0.0938x+3.1667\\ y&=-0.1635x+1.2461;\\ y&=-0.175x+1.338 \end{aligned} \quad [3]$$

respectively, where x is the agarose concentration, y is the relative signal (normalized to the isotonic NaCl solution).

The resulting relative signal-based formulas were applied to MRI machines from various vendors.

We observed a direct correlation between the relative MR signal intensity on T1WI and the volume of the contrast agent at a constant agarose concentration. There was an inverse dependence of the relative MR signal intensity on T2WI on the agarose concentration at a constant contrast agent concentration. Altering the agarose gel concentration allows mimicking of the T2 relaxation time of human tissue. The latter depends on the agarose amount and is independent of the concentration of other additives. However, the T1 relaxation time of agarose gels is not comparable with that of human tissue. Changing the T1 relaxation time of agarose gels requires adding a Gd^{+3}-based contrast agent. Carrageenan gels are elastic and ensure structural rigidity of the composition. Adding carrageenan to agarose gels solves the problem of low viscosity. For filling the 3D-printed model we prepared the compositions to make the T1 and T2 relaxation times similar to those of the corresponding control tissues; their description is provided in *Table 2*.

Figure 4 shows a photo of the printed mold and the phantom filled with tissue-mimicking compounds. The mold was filled gradually, starting with the more viscous structures (i.e., mixtures of carrageenan and agarose), followed by agarose hydrogels and emulsions, and finally the isotonic solution. The stomach, bladder, and brain were isolated with moisture-resistant Parafilm M elastic film, which prevents water evaporation from the hydrogels and accidental liquid mixture.

The phantom body hosts a special compartment for image quality control. The high-contrast spatial resolution is measured based on the intensity profiles of high-contrast objects of certain sizes. For this, a cylindrical insert (a test rod engraved with standard stripes or sectors) was made on a stereolithography 3D printer from a non-contrast material with holes and gaps of certain sizes in-between. To control

Table 2 Compositions for filling the fetal phantom

No.	Mimicked tissue	Composition
1	White matter of the brain	Oil-in-water emulsion with 40% fat phase concentration
2	Lungs	Hydrogel 0.3%, agarose + 0.33 M contrast agent
3	Bladder	Hydrogel 0.1%, agarose + 0.02 M contrast agent
4	Fetal muscles	Hydrogel 3% carrageenan + 0.5% agarose + 0.17 M contrast agent
5	Stomach	Hydrogel 0.1%, agarose + 0.02 M contrast agent
6	Maternal muscles	Hydrogel 3% carrageenan + 0.6% agarose + 0.11 M contrast agent
7	Liver	Hydrogel 0.6%, agarose + 0.22 M contrast agent
8	Amniotic fluid	Isotonic solution

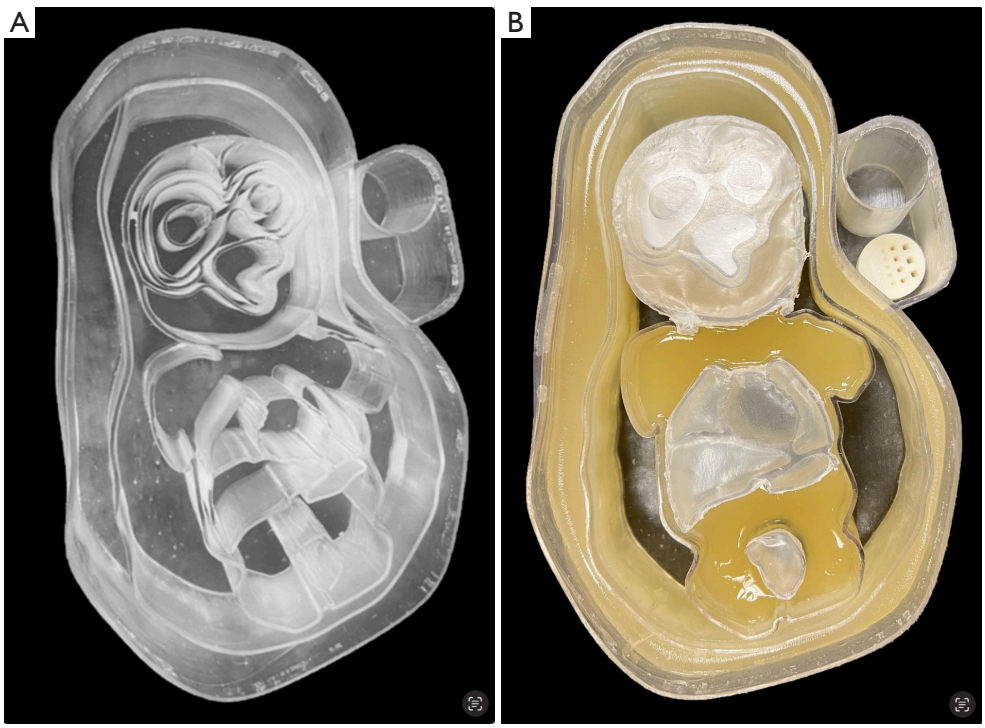

Figure 4 3D printed model of a fetal phantom: (A) overview, (B) test object filled with tissue-mimicking compositions. 3D, three-dimensional.

the image quality, the lower part of the compartment hosts an insert filled with an isotonic solution for assessing high-contrast spatial resolution, while vegetable oil is poured into the upper part.

The filled phantom is sealed with a lid that fits tightly and can be opened when necessary to update/replace the tissue-simulating compounds.

The resulting phantom was put into a refrigerator and scanned every 2 weeks over 6 months to monitor the stability of the relaxation times. Deterioration was observed only after 5.5 months.

The phantom scan results are presented in *Figure 5* and *Table 3*.

The Mann-Whitney test did not reveal significant differences in the signals from the pregnant woman and the phantom (P value >0.05).

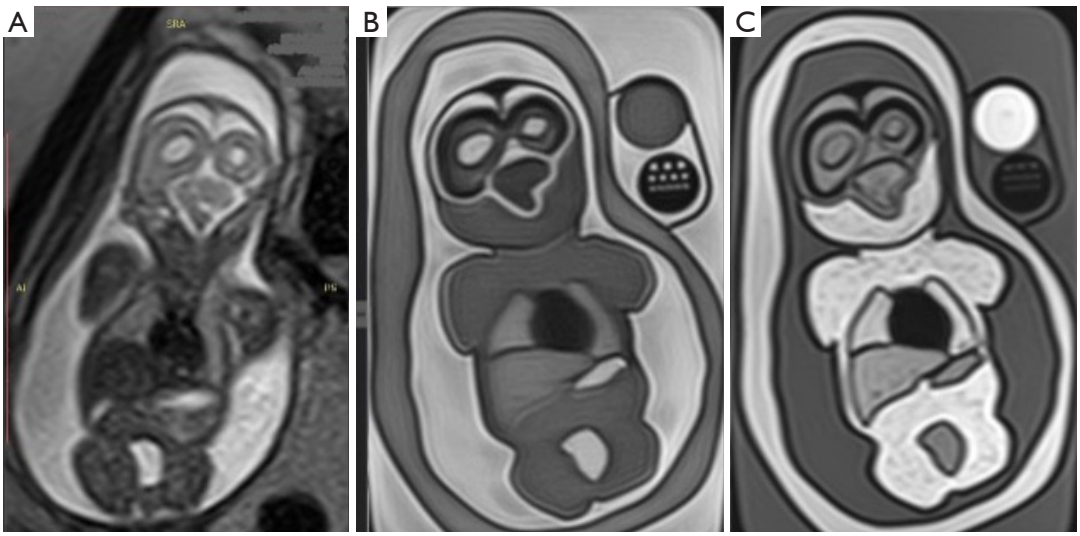

Figure 5 Scans: (A) T2WI of the fetus, (B) T2WI of the fetal phantom, (C) T1WI of the fetal phantom. T2WI, T2-weighted image; T1WI, T1-weighted image.

Table 3 Comparison of absolute and relative signal values from a pregnant woman at 20 weeks and 3 days and a fetal phantom

Tissue	MRI SI_{tissue}			MRI $SI_{rel.tissue}$ according Eq. [1]		
	T2	T1	T2FS	T2	T1	T2FS
Fetus						
White matter	3,073	1,372	3,545	0.41	1.24	0.49
Lung	3,353	1,161	3,580	0.45	1.05	0.49
Liver	1,156	1,682	838	0.15	1.52	0.12
Bladder	4,418	1,007	5,430	0.59	0.91	0.75
Maternal muscles	367	1,023	272	0.05	0.92	0.04
Fetal muscles	1,232	1,141	1,226	0.16	1.03	0.17
Isotonic solution placed next to the pregnant women	7,468	1,107	7,246	1	1	1
Phantom						
White matter	2,373	2,104	2,309	0.33	1.52	0.35
Lung	3,524	1,841	3,431	0.49	1.33	0.52
Liver	1,222	2,380	924	0.17	1.72	0.14
Bladder	5,609	1,536	5,344	0.78	1.11	0.81
Maternal muscles	863	1,592	726	0.12	1.15	0.11
Fetal muscles	2,373	1,605	2,376	0.33	1.16	0.36
Isotonic solution inside the phantom	7,191	1,384	6,598	1	1	1

MRI, magnetic resonance imaging; SI_{tissue}, signal intensity of the tissue; $SI_{rel.tissue}$, relative magnetic resonance signal of tissue, relative units; T1, spin-lattice relaxation time; T2, spin-spin relaxation time; T2FS, T2 with fat suppression.

Discussion

We designed the compositions to mimic the maturing white matter of the brain, lungs, stomach, liver, bladder, fetal muscles, and maternal muscles. The MRI signal intensities (T1, T2, T2FS) closely matched those of the corresponding fetal tissues at 20 weeks 3 days of gestation. The measurements show no significant discrepancy and correspond to what was observed *in vivo*.

Although the fetus moves during MRI, only when it is motionless (or the region of interest is motionless) can the most informative image series be obtained. Thus, setting up protocols requires minimizing the pulse sequence time for the smallest field of view while maintaining optimal image quality (optimal signal-to-noise ratio and spatial resolution). To address this challenge, incorporating motor activity into the phantom is not advisable at this stage. Simulations of motor activity for the fetus' individual parts will be added on the next stage.

The phantom can be used for MRI scanning in T1 and T2 modes to test the stability of parameters and to obtain metrologically sound measurements (31,32). Phantom modelling allows testing the existing scanning protocols to standardize data acquisition and set coefficients that would normalize the obtained values. This technique is crucial for those wishing to participate in multi-center studies or conduct complex imaging methods such as texture analysis.

Conclusions

In the present study, an anthropomorphic fetal phantom was constructed and filled with compositions to simulate the features of the fetal organs. The proposed methodology can be used during the critical project phase involving the simulation of a moving anthropomorphic 3D phantom of a fetus in the uterus. The phantom can be used to train doctors and MRI technicians, as well as to assess and verify equipment performance in routine clinical practice. Our test object will help gain core skills in setting up and using various scanning protocols to optimize the pulse sequence duration and the quality of the resulting fetal MRI images.

Acknowledgments

Funding: This paper was supported by a group of authors as a part of the research and development effort titled "Research program to further the standardization, safety and quality of magnetic resonance imaging", (USIS No. 123031500007-6) in accordance with the Order No. 1196 dated December 21, 2022 "On approval of state assignments funded by means of allocations from the budget of the city of Moscow to the state budgetary (autonomous) institutions subordinate to the Moscow Health Care Department, for 2023 and the planned period of 2024 and 2025" issued by the Moscow Health Care Department.

Footnote

Reporting Checklist: The authors have completed the MDAR reporting checklist. Available at https://qims.amegroups.com/article/view/10.21037/qims-24-501/rc

Conflicts of Interest: All authors have completed the ICMJE uniform disclosure form (available at https://qims.amegroups.com/article/view/10.21037/qims-24-501/coif). The authors have no conflicts of interest to declare.

Ethical Statement: The authors are accountable for all aspects of the work in ensuring that questions related to the accuracy or integrity of any part of the work are appropriately investigated and resolved. The study was conducted in accordance with the Declaration of Helsinki (as revised in 2013). The study was approved by independent ethics committee of State Budget-Funded Health Care Institution of the City of Moscow "Research and Practical Clinical Center for Diagnostics and Telemedicine Technologies of the Moscow Health Care Department" (N06/2023 from September 21, 2023). Informed consent for the use of anonymized images for academic purposes was obtained.

References

1. Ni Q, Zhang Y, Wen T, Li L. A Sparse Volume Reconstruction Method for Fetal Brain MRI Using

Adaptive Kernel Regression. Biomed Res Int 2021;2021:6685943.
2. Vasilev YA, Bazhin AV, Masri AG, Vasileva YN, Panina OY, Sinitsyn VE. Chest MRI of a pregnant woman with COVID-19 pneumonia. Digital Diagnostics 2020;1:61-8.
3. Bulas D, Egloff A. Benefits and risks of MRI in pregnancy. Semin Perinatol 2013;37:301-4.
4. Committee Opinion No. 723: Guidelines for Diagnostic Imaging During Pregnancy and Lactation. Obstet Gynecol 2017;130:e210-6.
5. Pugash D, Brugger PC, Bettelheim D, Prayer D. Prenatal ultrasound and fetal MRI: the comparative value of each modality in prenatal diagnosis. Eur J Radiol 2008;68:214-26.
6. Coakley FV, Glenn OA, Qayyum A, Barkovich AJ, Goldstein R, Filly RA. Fetal MRI: a developing technique for the developing patient. AJR Am J Roentgenol 2004;182:243-52.
7. Shulman M, Cho E, Aasi B, Cheng J, Nithiyanantham S, Waddell N, Sussman D. Quantitative analysis of fetal magnetic resonance phantoms and recommendations for an anthropomorphic motion phantom. MAGMA 2020;33:257-72.
8. Cheung CL, Looi T, Drake J, Kim P. Magnetic resonance imaging properties of multimodality anthropomorphic silicone rubber phantoms for validating surgical robots and image guided therapy systems. Proceedings of SPIE - The International Society for Optical Engineering 2012;8316:67.
9. Victoria T, Jaramillo D, Roberts TP, Zarnow D, Johnson AM, Delgado J, Rubesova E, Vossough A. Fetal magnetic resonance imaging: jumping from 1.5 to 3 tesla (preliminary experience). Pediatr Radiol 2014;44:376-86; quiz 373-5.
10. Kording F, Schoennagel BP, de Sousa MT, Fehrs K, Adam G, Yamamura J, Ruprecht C. Evaluation of a Portable Doppler Ultrasound Gating Device for Fetal Cardiac MR Imaging: Initial Results at 1.5T and 3T. Magn Reson Med Sci 2018;17:308-17.
11. Jansz MS, Seed M, van Amerom JF, Wong D, Grosse-Wortmann L, Yoo SJ, Macgowan CK. Metric optimized gating for fetal cardiac MRI. Magn Reson Med 2010;64:1304-14.
12. Goolaub DS, Roy CW, Schrauben E, Sussman D, Marini D, Seed M, Macgowan CK. Multidimensional fetal flow imaging with cardiovascular magnetic resonance: a feasibility study. J Cardiovasc Magn Reson 2018;20:77.
13. Chen Q, Xie G, Luo C, Yang X, Zhu J, Lee J, Su S, Liang D, Zhang X, Liu X, Li Y, Zheng H. A Dedicated 36-Channel Receive Array for Fetal MRI at 3T. IEEE Trans Med Imaging 2018;37:2290-7.
14. Garel C. Fetal MRI: what is the future? Ultrasound Obstet Gynecol 2008;31:123-8.
15. McIlvain G, Ganji E, Cooper C, Killian ML, Ogunnaike BA, Johnson CL. Reliable preparation of agarose phantoms for use in quantitative magnetic resonance elastography. J Mech Behav Biomed Mater 2019;97:65-73.
16. Chen SJ, Hellier P, Marchal M, Gauvrit JY, Carpentier R, Morandi X, Collins DL. An anthropomorphic polyvinyl alcohol brain phantom based on Colin27 for use in multimodal imaging. Med Phys 2012;39:554-61.
17. Morozov S, Sergunova K, Petraikin A, Akhmad E, Kivasev S, Semenov D, Blokhin I, Karpov I, Vladzymyrskyy A, Morozov A. Diffusion processes modeling in magnetic resonance imaging. Insights Imaging 2020;11:60.
18. Antoniou A, Damianou C. MR relaxation properties of tissue-mimicking phantoms. Ultrasonics 2022;119:106600.
19. Gillmann C, Homolka N, Johnen W, Runz A, Echner G, Pfaffenberger A, Mann P, Schneider V, Hoffmann AL, Troost EGC, Koerber SA, Kotzerke J, Beuthien-Baumann B. Technical Note: ADAM PETer - An anthropomorphic, deformable and multimodality pelvis phantom with positron emission tomography extension for radiotherapy. Med Phys 2021;48:1624-32.
20. Howe FA. Relaxation times in paramagnetically doped agarose gels as a function of temperature and ion concentration. Magn Reson Imaging 1988;6:263-70.
21. Mitchell MD, Kundel HL, Axel L, Joseph PM. Agarose as a tissue equivalent phantom material for NMR imaging. Magn Reson Imaging 1986;4:263-6.
22. Hellerbach A, Schuster V, Jansen A, Sommer J. MRI phantoms - are there alternatives to agar? PLoS One 2013;8:e70343.
23. Kraft KA, Fatouros PP, Clarke GD, Kishore PR. An MRI phantom material for quantitative relaxometry. Magn Reson Med 1987;5:555-62.
24. Niebuhr NI, Johnen W, Güldaglar T, Runz A, Echner G, Mann P, Möhler C, Pfaffenberger A, Jäkel O, Greilich S. Technical Note: Radiological properties of tissue surrogates used in a multimodality deformable pelvic phantom for MR-guided radiotherapy. Med Phys 2016;43:908-16.
25. De Brabandere M, Kirisits C, Peeters R, Haustermans K, Van den Heuvel F. Accuracy of seed reconstruction in prostate postplanning studied with a CT- and MRI-compatible phantom. Radiother Oncol 2006;79:190-7.

26. Woletz M, Roat S, Hummer A, Tik M, Windischberger C. Technical Note: Human tissue-equivalent MRI phantom preparation for 3 and 7 Tesla. Med Phys 2021;48:4387-94.
27. Ohno S, Kato H, Harimoto T, Ikemoto Y, Yoshitomi K, Kadohisa S, Kuroda M, Kanazawa S. Production of a human-tissue-equivalent MRI phantom: optimization of material heating. Magn Reson Med Sci 2008;7:131-40.
28. Hattori K, Ikemoto Y, Takao W, Ohno S, Harimoto T, Kanazawa S, Oita M, Shibuya K, Kuroda M, Kato H. Development of MRI phantom equivalent to human tissues for 3.0-T MRI. Med Phys 2013;40:032303.
29. Garcia-Polo P, Gagoski B, Guerin B, Gale E, Adalsteinsson E, Grant PE, Wald LL. An anthropomorphic MR phantom of the gravid abdomen including the uterus, placenta, fetus and fetal brain. International Society for Magnetic Resonance in Medicine 2015. Available online: https://cds.ismrm.org/protected/15MProceedings/PDFfiles/1545.pdf
30. Filippou V, Tsoumpas C. Recent advances on the development of phantoms using 3D printing for imaging with CT, MRI, PET, SPECT, and ultrasound. Med Phys 2018;45:e740-60.
31. State Budget-Funded Health Care Institution of the City of Moscow "Research and Practical Clinical Center for Diagnostics and Telemedicine Technologies of the Moscow Health Care Department" (2022). Metodika kontrolya parametrov i xarakteristik magnitno-rezonansny`x tomografov v usloviyax e`kspluatacii [Control over parametes and features of MRI scanners during routine operation]. Moscow: State Budget-Funded Health Care Institution of the City of Moscow "Research and Practical Clinical Center for Diagnostics and Telemedicine Technologies of the Moscow Health Care Department" Research and Practical Clinical Center for Diagnostics and Telemedicine Technologies of the Moscow Health Care Department, Moscow, 24 building 1 Petrovka St., Moscow, the Russian Federation, 2022 – P. 80 – Series "The best practices of radiology and instrumental diagnostics" – ISBN 26187124. Available online: https://elibrary.ru/item.asp?id=49743767
32. Certificate for state registration of computer software No. 2018619223, the Russian Federation. Application for control over the quality of the parameters of magnetic resonance imaging: No. 2018616671: submitted 27.06.2018: published 02.08.2018. Sergunova KA, Akhmad ES, Vladzymyrskyy AV, Morozov SP; submitter State Budget-Funded Health Care Institution of the City of Moscow "Research and Practical Clinical Center for Diagnostics and Telemedicine Technologies of the Moscow Health Care Department". Available online: https://elibrary.ru/item.asp?id=39299389

Cite this article as: Cherkasskaya MV, Syrkashev EM, Sokolova MV, Petraikin AV, Semenov DS, Vasilev YA. Development of fetal magnetic resonance imaging (MRI) phantom. Quant Imaging Med Surg 2024;14(9):6250-6259. doi: 10.21037/qims-24-501

